

Crustal Structure Across the Western Afar Margin from the Uplifted Plateau to the Rift Axis using Receiver Functions

Abdulhakim Ahmed¹, Cecile Doubre¹, Sylvie Leroy², Derek Keir^{3,4}, Carolina Pagli^{5,6}, Hammond O. S. James⁷

¹ Université de Strasbourg, CNRS-INSU, IPGS-UMR 7516, F-67000 Strasbourg, France.
² Sorbonne Université, CNRS-INSU, Institut des Sciences de la Terre de Paris, ISTEP, Paris, France.
³ School of Ocean and Earth Science, University of Southampton, Southampton, United Kingdom.
⁴ Dipartimento di Scienze della Terra, Università degli Studi di Firenze, Florence, Italy.
⁵ School of Earth and Environment, University of Leeds, Leeds, UK.
⁶ Dipartimento di Scienze della Terra, Università di Pisa, Pisa, Italy.
⁷ Department of Earth and Planetary Sciences, Birkbeck, University of London – UK.

Introduction

The subaerial rift elevation of the Afar Depression, where the transition from continental rifting to sea floor spreading occur, offers unique opportunities to address how the rifting processes have evolved during the continental breakup. The continental rifting in Afar started in the Oligo-Miocene and associated with the development of steep border fault systems (Wolfe et al., 2005; Stab et al., 2016). Followed by eastward migration of the rifting toward the rift axis where magma intrusion is thought to accommodate the majority of extension (e.g. Wright et al., 2006; Grandin et al., 2010).

Higher resolution images of lithospheric structure across the western Afar margin can provide insights to constrain the tectonic and magmatic processes that are involved in rift evolution. In particular, the key questions are:
 - Is the strain migration from the stable plateau to the rift axis continuous and progressive or there are jumps in strain localization during rifting?
 - What is the role of the magmatic intrusions in the development of the Afar rift (Buck, 2006)?

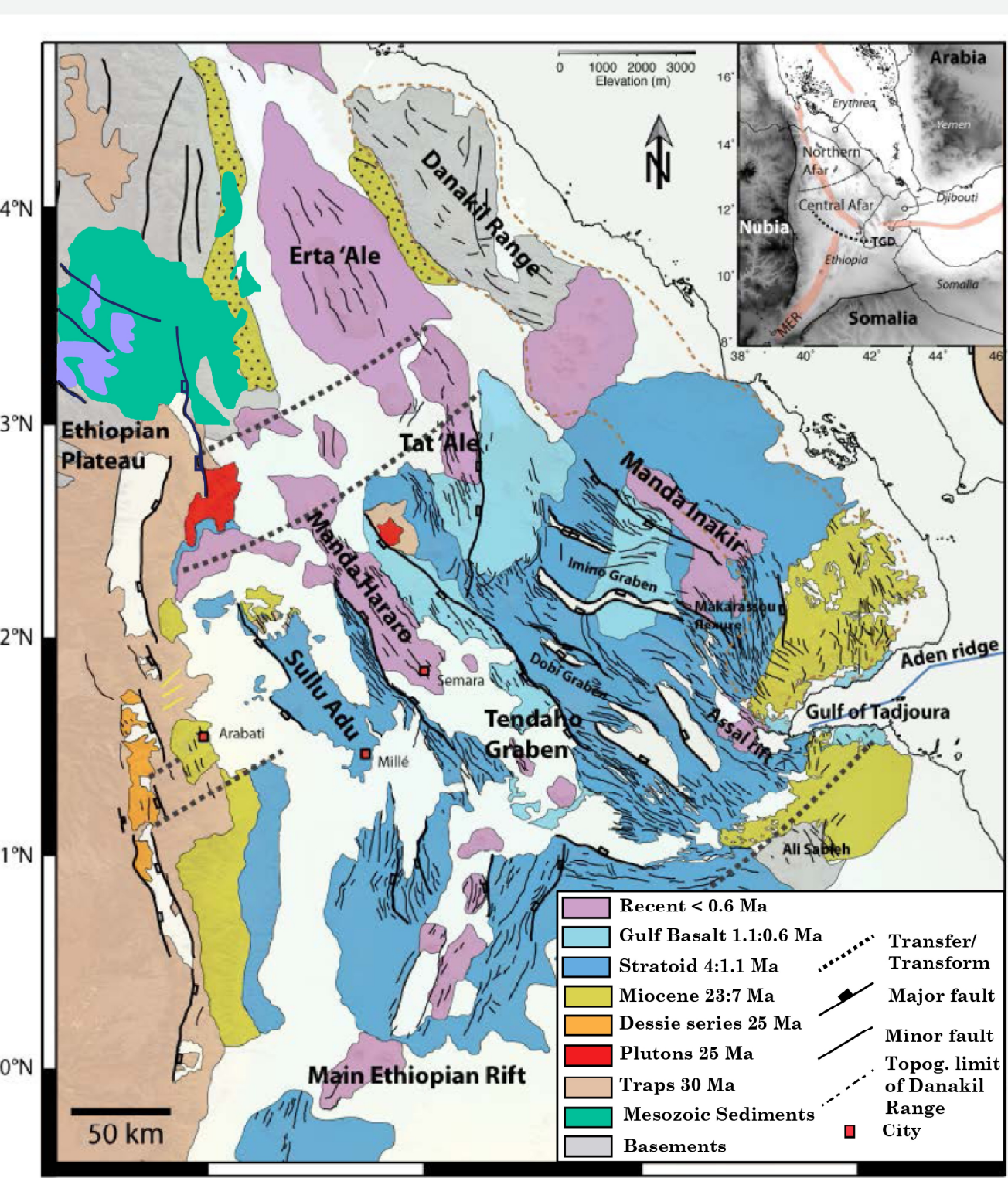
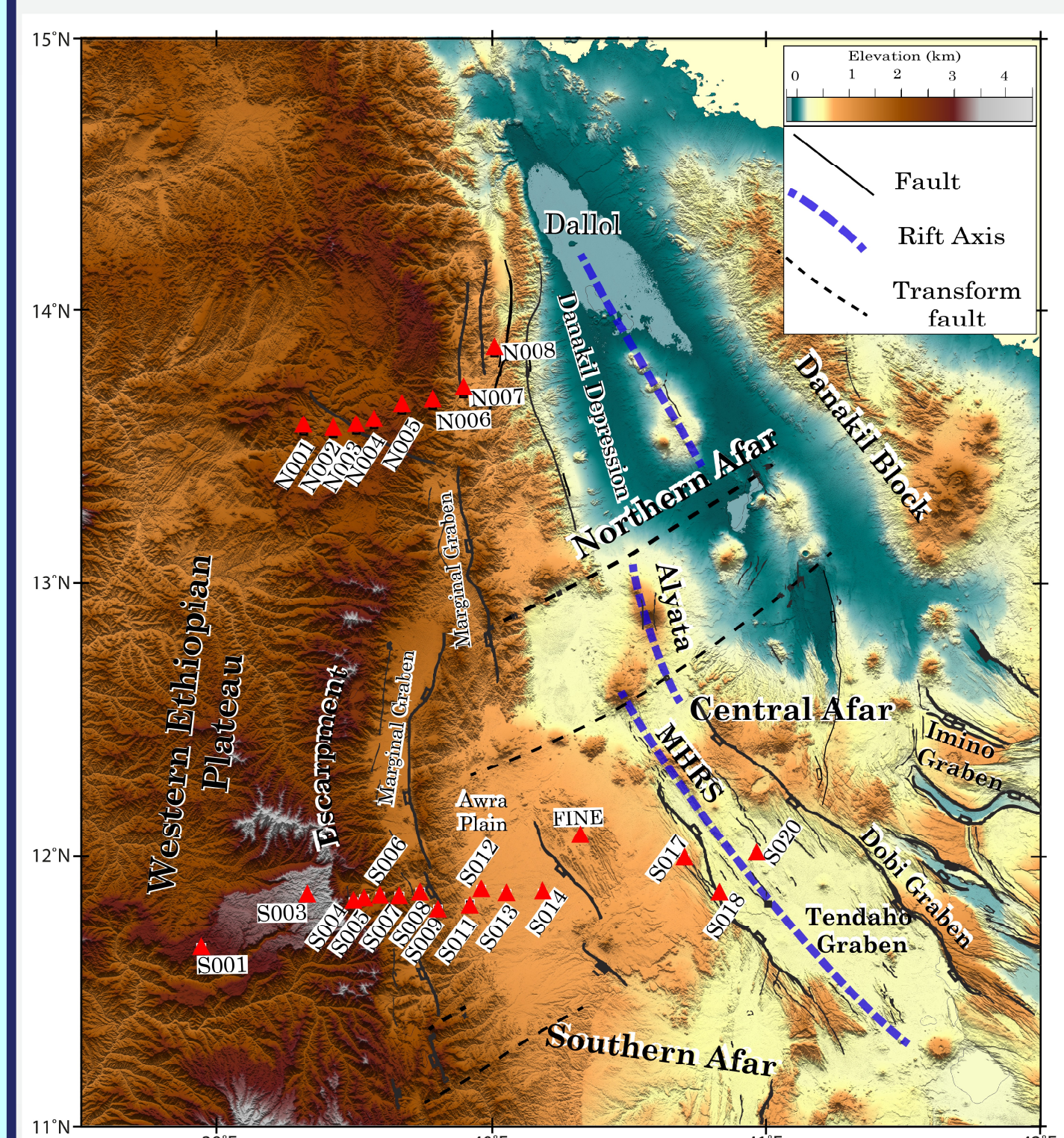


Fig. (1) Topographical map of the study area showing the main tectonic structures and the location of the seismic stations (red triangles) along two profiles. MHR: Manda Harraro Rift Segment.

Fig. (2) Geological and structural map of the Afar Depression and surrounding highlands modified from Stab et al. (2016). Inset at the upper right corner is a regional map showing the location of the study area.

Data & Method

- A seismic monitoring project was carried out to study the crustal structure and seismic activity of Afar and its margins.
- The seismic network is consist of 29 broadband seismic stations deployed along two SW-NE profiles, from May 2017 until September 2018. During this time period more than 100 teleseismic events with epicentral distance ranging between 25°-90° and Mw > 5.5 were recorded by the array.
- The unstable operation of some stations resulted in reducing the actual number of events recorded and hence the number of stations used for final analysis. In addition, the inhomogeneous distribution of the seismic events with concentration to the E and NE prevented detailed anisotropy analysis.
- The actual number of events selected for the final analysis varies from 15 to 72 depending on the background noise and the data recovery of the station.
- We computed the Receiver Function (RF) using the iterative deconvolution method developed by Ligoria & Ammon (1999). The data set was inverted by the stacking method of Zhu & Kanamori (2000).
- Based on the results of the controlled-source experiments (e.g. Makris and Ginzburg, 1987), and the previous receiver functions studies (e.g. Hammond et al., 2011), we select an average crustal velocity $V_p = 6.3$ kms⁻¹ for the stations located on the western plateau and 6.0 kms⁻¹ for the stations located within the Afar rift.
- We employ the bootstrap resampling technique (Efron and Tibshirani 1986), to estimate the standard deviation for both crustal thickness H and V_p/V_s and to estimate the uncertainty coming from the average crustal P -wave velocity used in the inversions.



Fig. (3) Photo shows the deployment of the seismic stations.

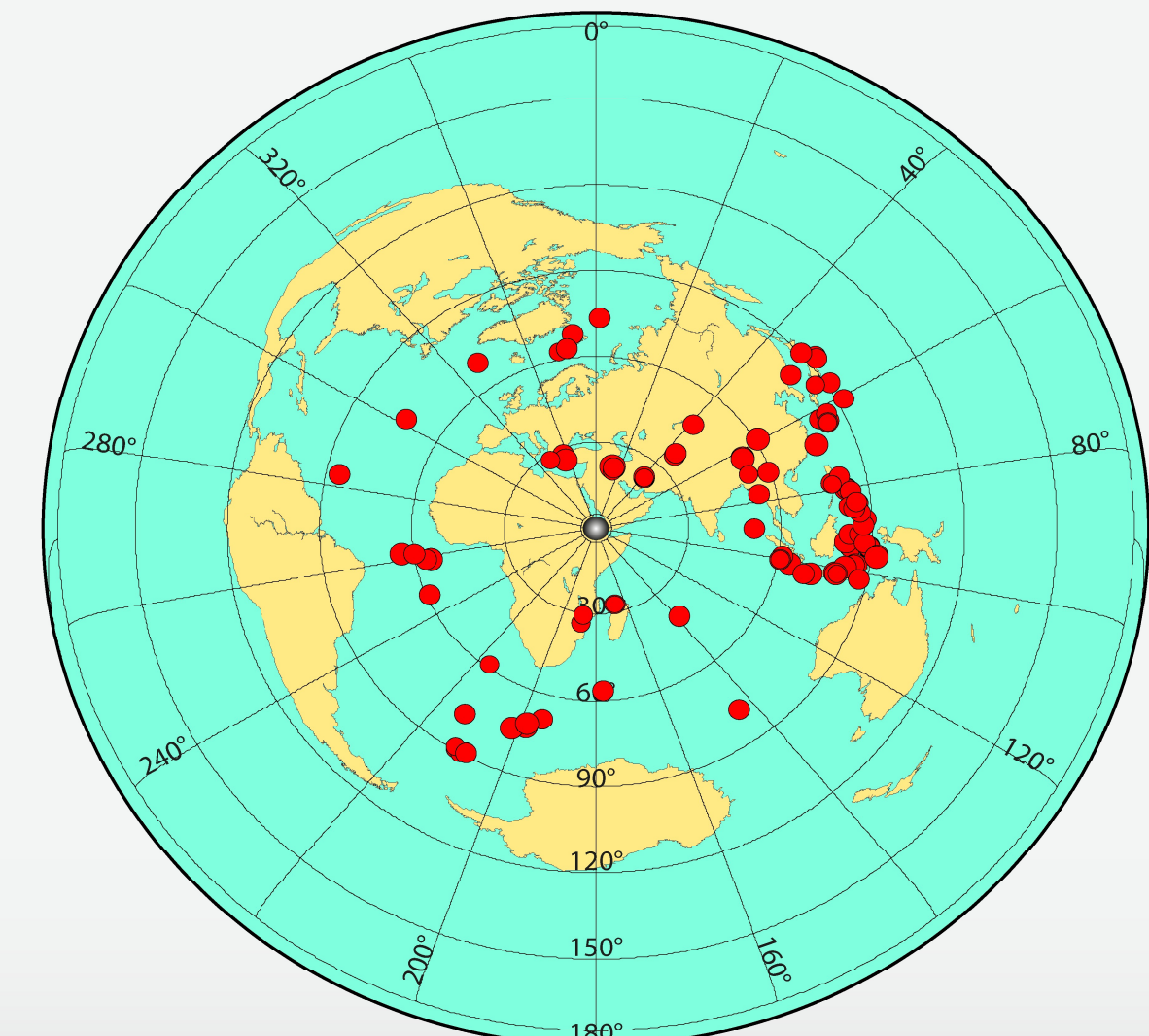


Fig. (4) map showing the distribution of the teleseismic events used in this study centered at the network location.

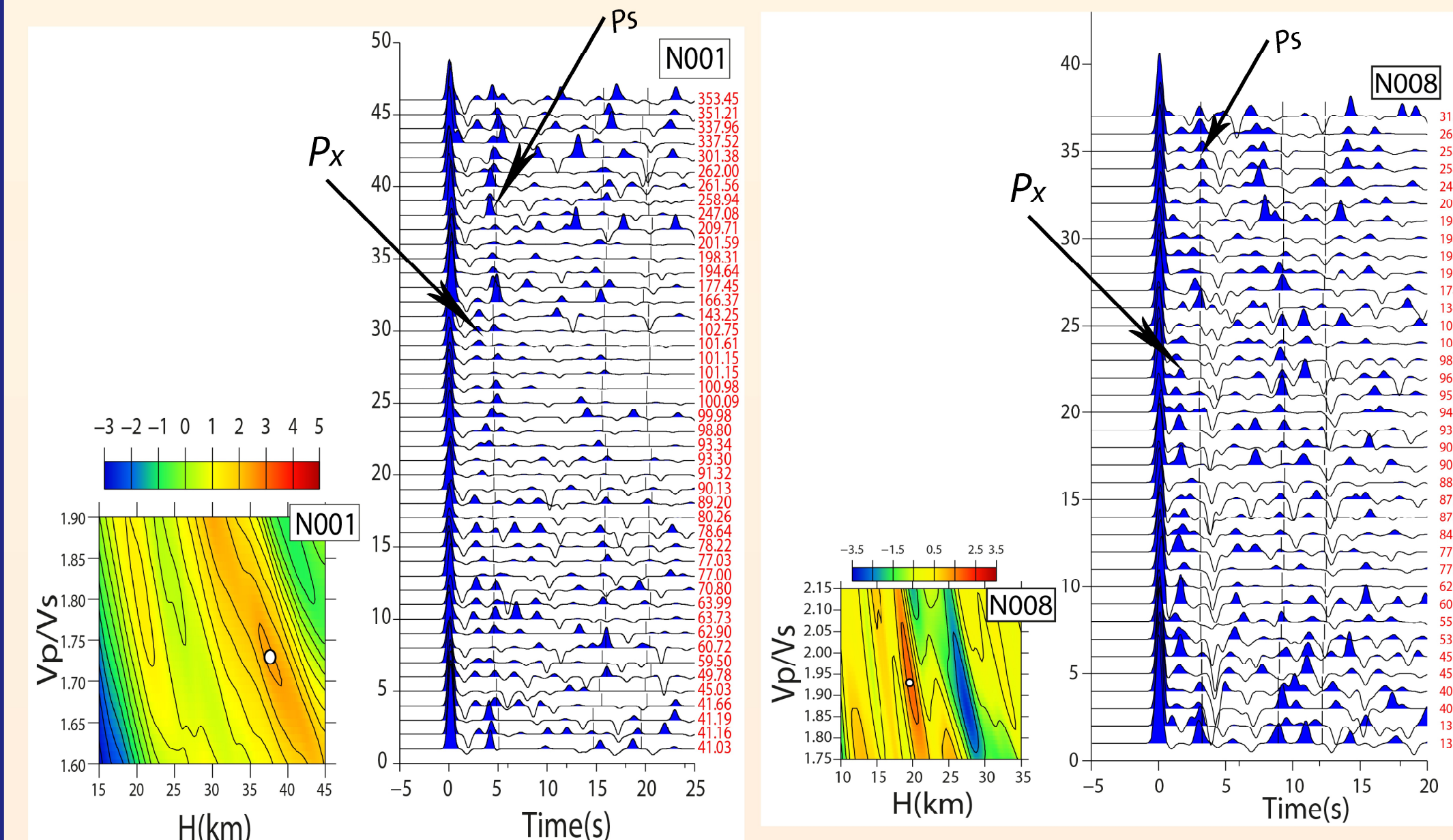


Fig. (5) Some of the RF results from the northern profile:

- At N001 station (on the western plateau of the northern profile) the crustal thickness was found to be 37.6 Km from stacked RF and V_p/V_s ratio 1.73.
- A comparable result was found for the stations N002-N006 that are located on the western plateau next to northern Afar with an average of 38 km.
- At N007 station located at the foothill area the crustal thickness decreases to about 24.0 Km and the V_p/V_s ratio is 1.79.
- The crustal thickness beneath N008 station is 19.6 km associated with high V_p/V_s ratio of 1.93.
- We notice a strong azimuthal effect on the RF, with very low PS amplitudes for events coming from the E and NE.
- A P_x conversion phase (intra-crustal phase) is clearly seen at most of the stations.
- The amplitude of the P_x conversion phase is also dependent on the backazimuth.

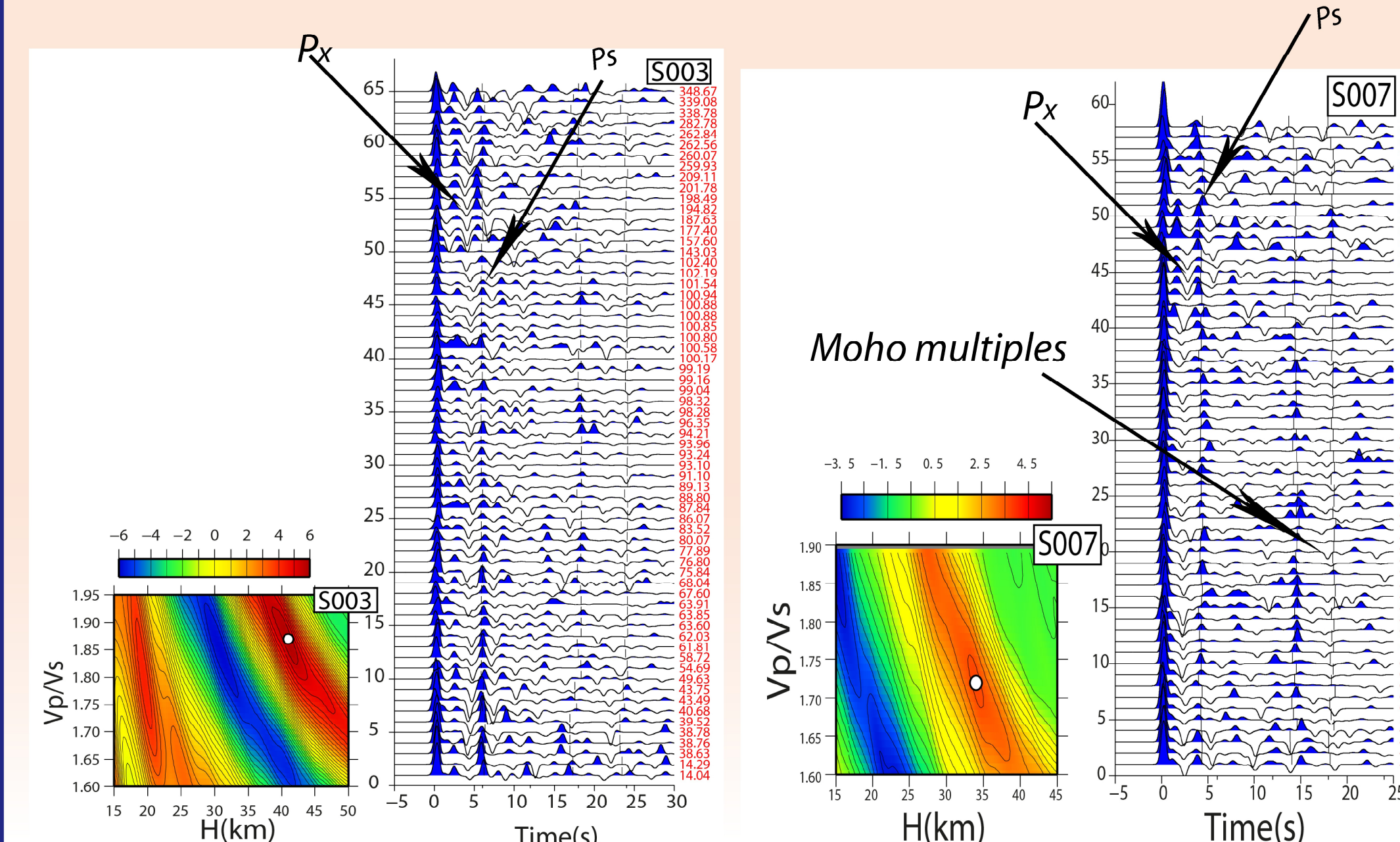


Fig. (6) Some of the RF results from the southern profile:

- The average crustal thickness of the western plateau next to central Afar is ~42 km as deduced from S001 and S003 stations.
- The crustal thickness decreases riftward reaching 19.8 at the rift axis.
- The V_p/V_s ratio of the western plateau surrounding central Afar and the marginal area is slightly elevated compared to the western plateau surrounding northern Afar.
- The azimuthal effect on the P_s amplitude for the stations that are located on the Plateau and marginal area is less than that noticed for the stations of the northern profile.
- We noticed a significant increase in the V_p/V_s ratios values (>1.9) coincident with crustal thinning toward the central axis of the rift.

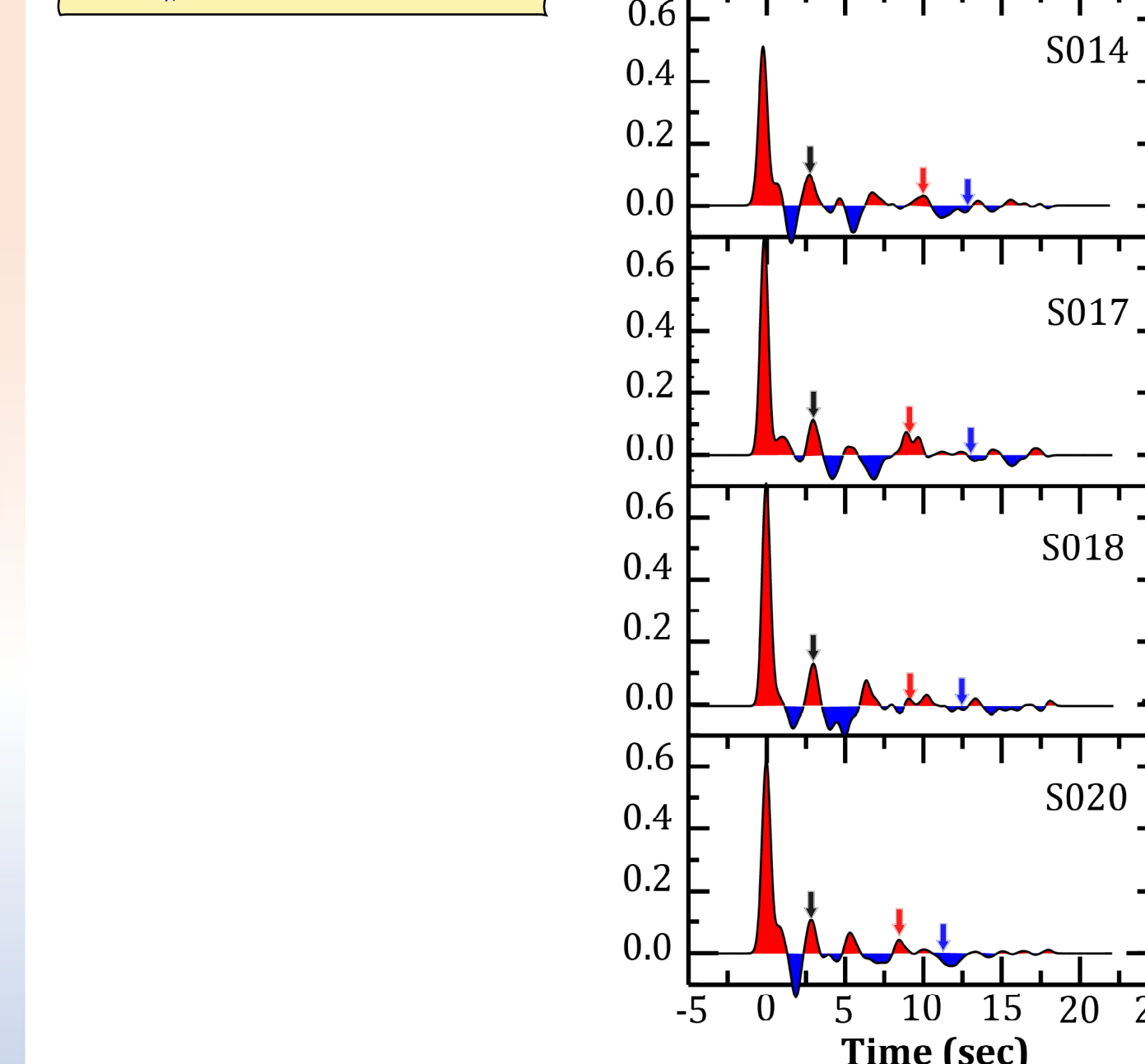
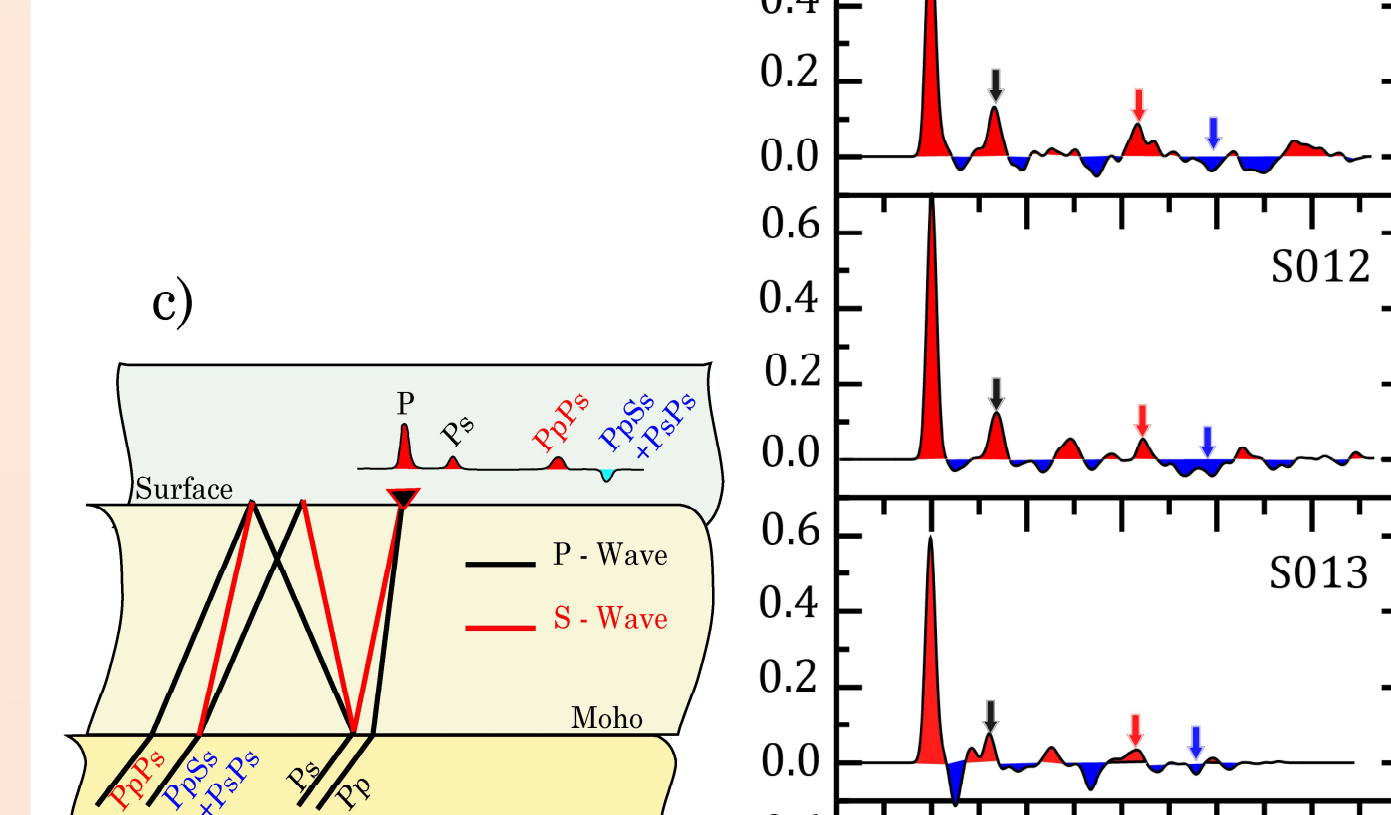
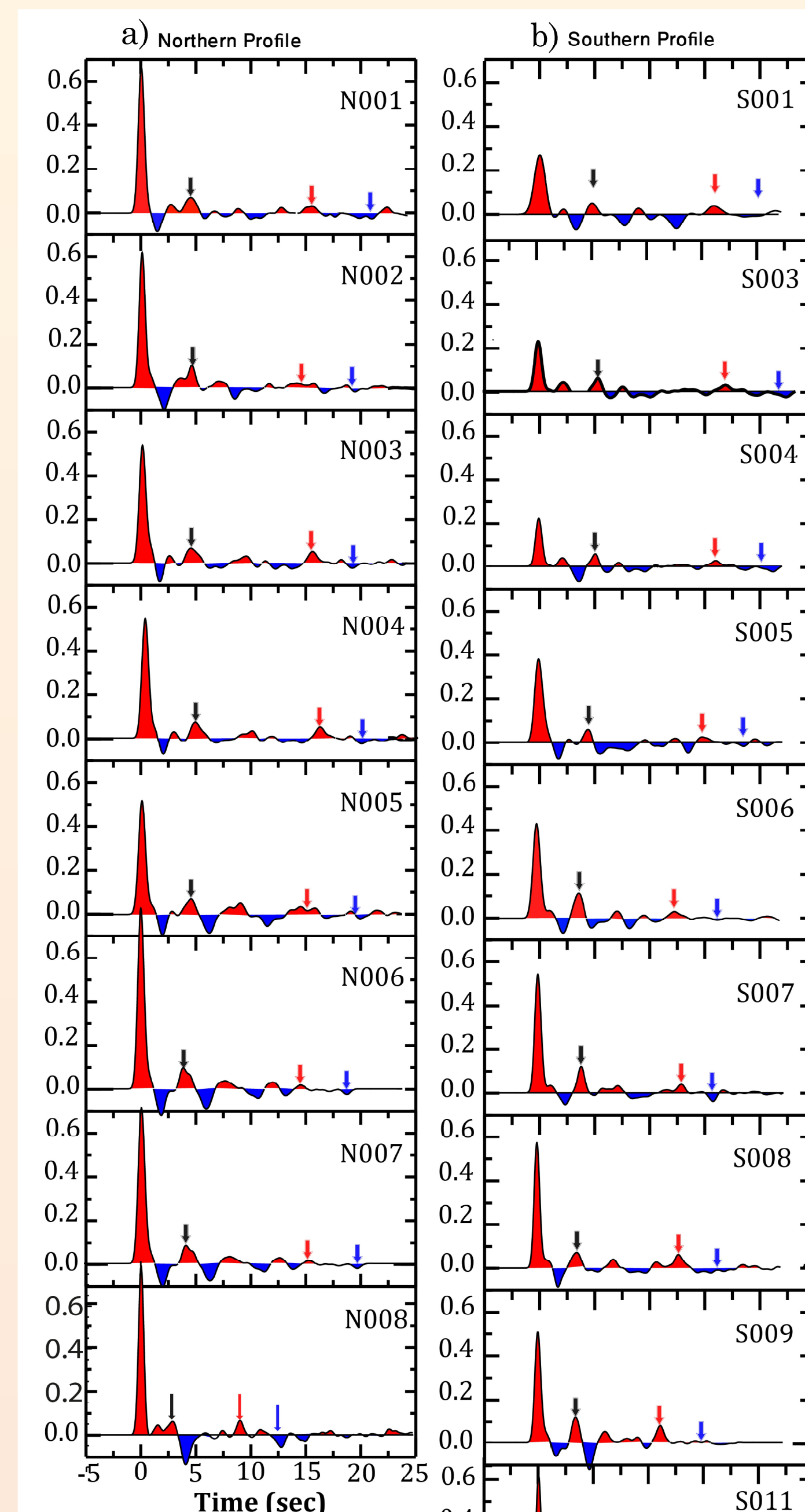


Fig. (7) Stacked receiver functions for the seismic stations along the two profiles. a) the northern profile - Danakil Depression, b) the southern profile at the latitude of the central Afar, and c) sketch illustrating the path of the converted phases and

Fig. (8) Map of crustal thicknesses (H) calculated using the H-k method; Topographical map with the crustal thickness variations across western Afar margin.

Fig. (9) Map of V_p/V_s ratio calculated using the H-k method; Topographical map with V_p/V_s ratio variations across western Afar margin.

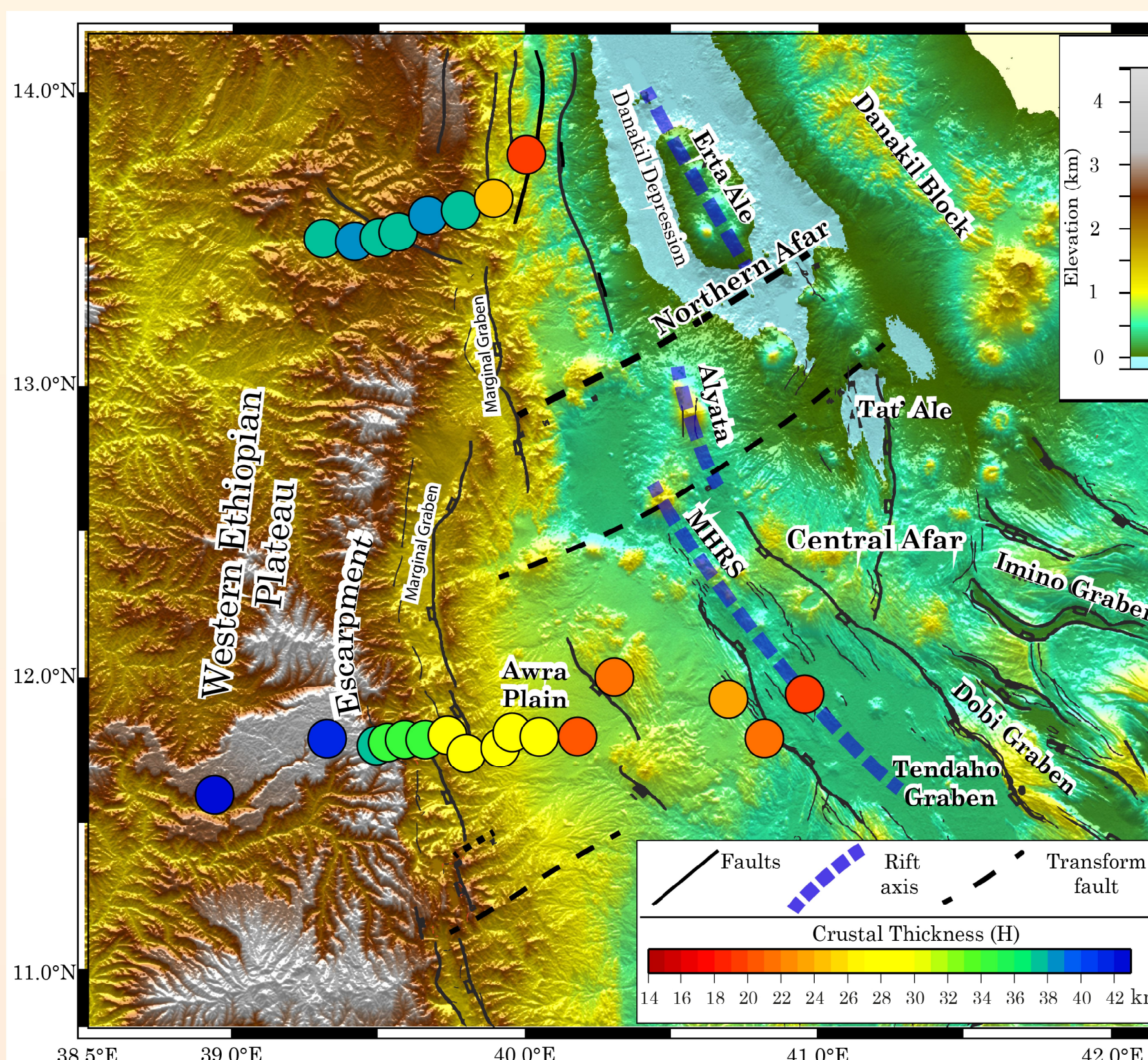


Fig. (10) The CCP migrated cross sections along the northern profile:
 - Topography along the profile (elevation scale vertically exaggerated).
 - The Moho depth estimated from H-k stacking method and corrected for the station altitude is plotted with the small circles.
 - The errors in Moho depth estimated from bootstrap methods is represented by the vertical bars.
 - The Moho depth is in the range ~ 35-19.0 km.
 - We estimate the maximum crust thinning occurs between S006 and S007 stations to be ~14 Km in about 10 Km horizontal distance.

- Thinning of the crust eastward from the high plateau to the rift axis.
- Four distinct regions of uniform crustal thickness along the southern profile.
- Thinner crust along the northern profile compared to the southern profile.

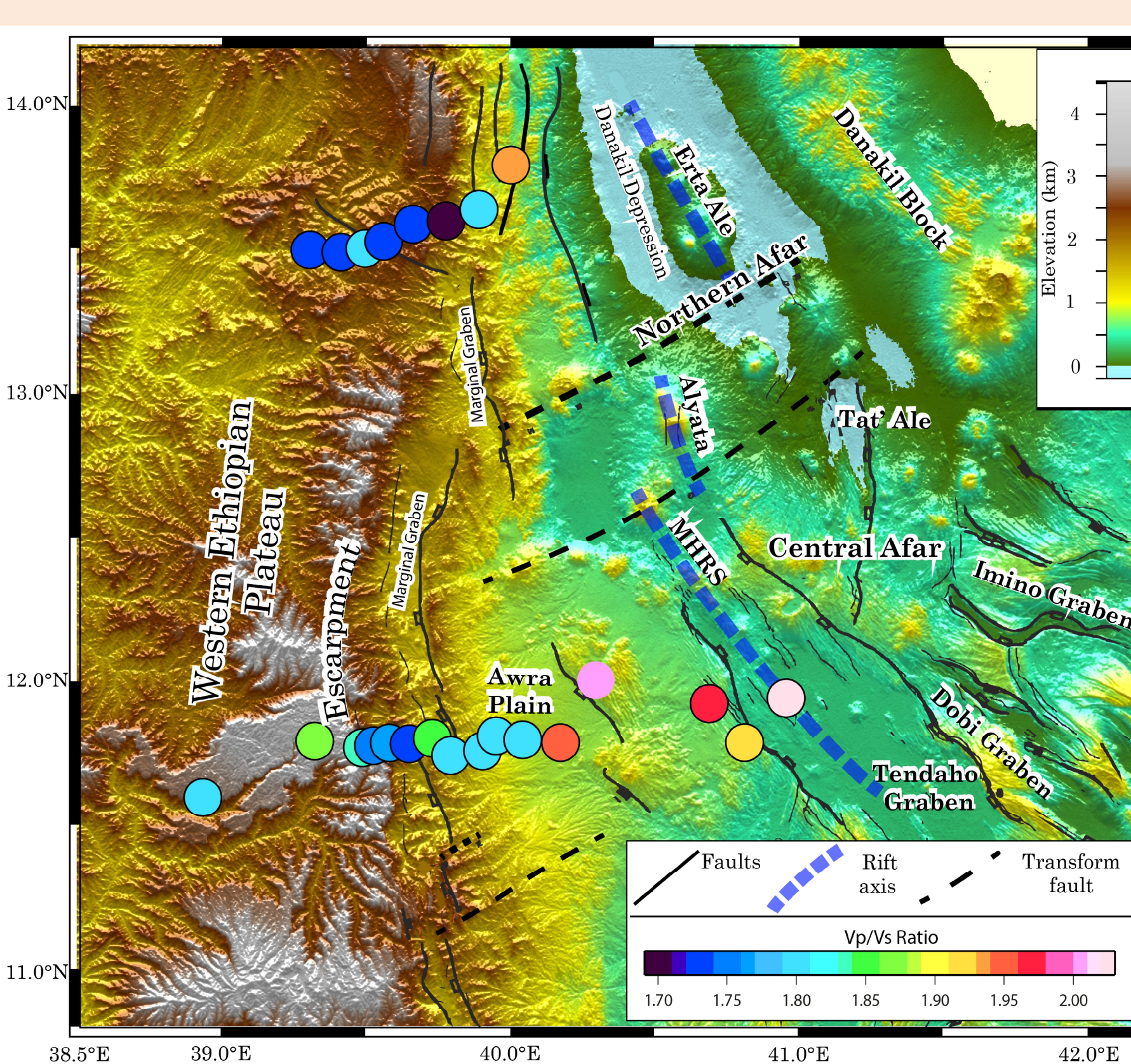


Fig. (11) The CCP migrated cross section along the southern profile:
 - The Moho depth is in the range ~ 40-19.0 km.
 - We estimate the crust thinning occurs in 4 steps along the profile between the stations S003-S005, S007-S008 and S013-S014.
 - These 4 steps divided the area between the western plateau and the rift axis to four distinct regions of uniform crustal thickness.
 - A clear intra-crustal interface could be seen along the profile.

- Higher V_p/V_s ratios toward the rift axis (thinner crust).
- For the northern profile the stations that are located near the faults shows slightly elevated V_p/V_s ratios.
- For the southern profile slightly elevated V_p/V_s ratios for the stations located on the western Plateau and marginal area.

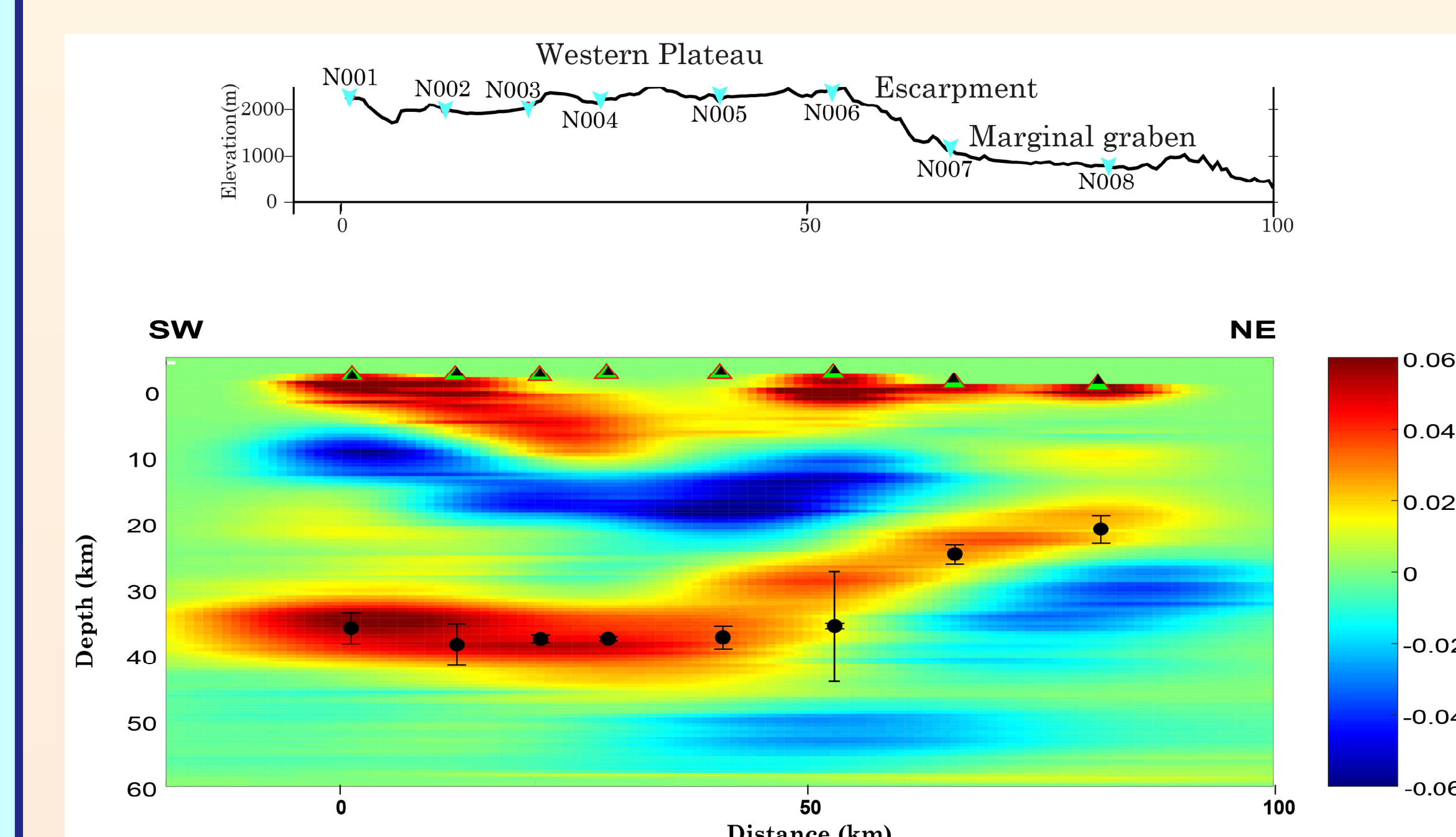


Fig. (10) The CCP migrated cross sections along the northern profile:
 - Topography along the profile (elevation scale vertically exaggerated).
 - The Moho depth estimated from H-k stacking method and corrected for the station altitude is plotted with the small circles.
 - The errors in Moho depth estimated from bootstrap methods is represented by the vertical bars.
 - The Moho depth is in the range ~ 35-19.0 km.
 - We estimate the maximum crust thinning occurs between S006 and S007 stations to be ~14 Km in about 10 Km horizontal distance.

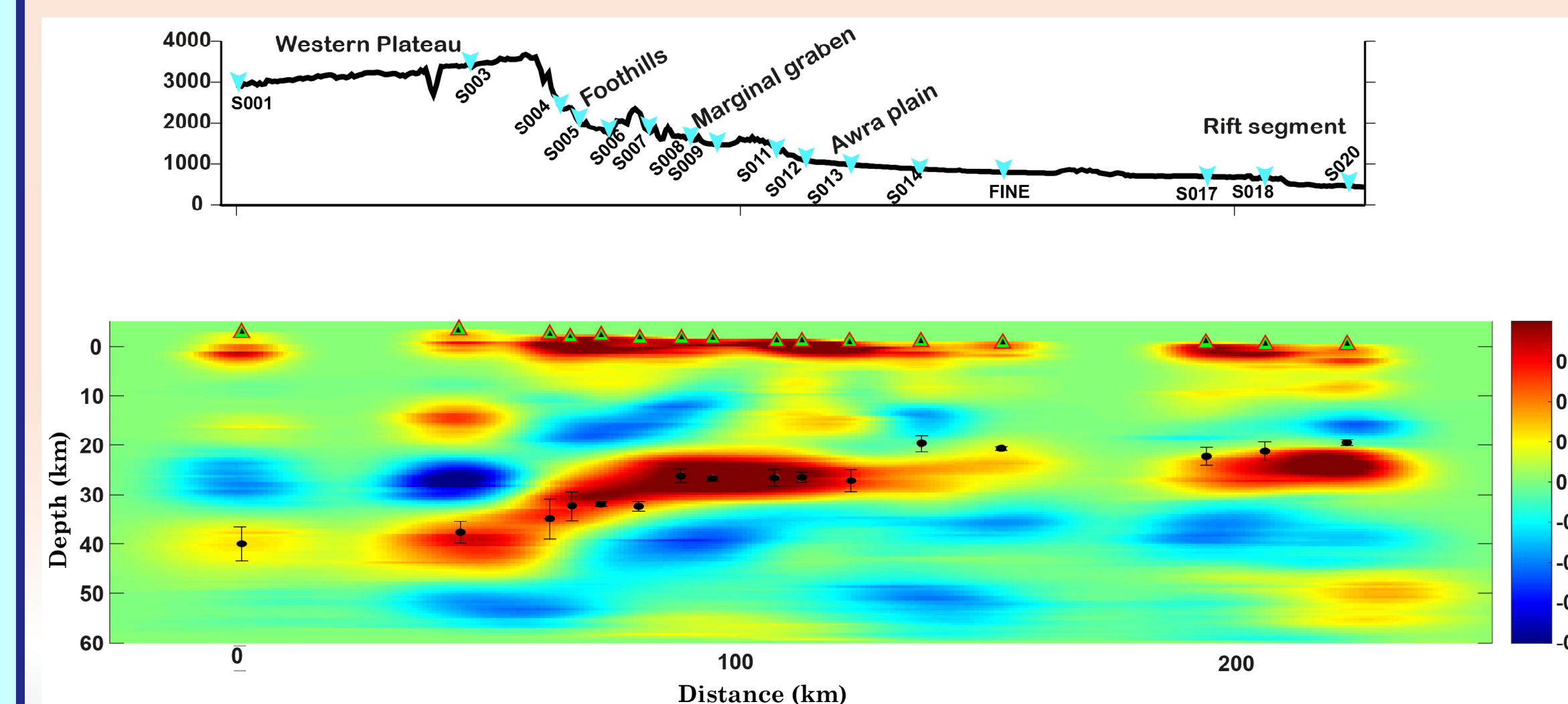


Fig. (11) The CCP migrated cross section along the southern profile:
 - The Moho depth is in the range ~ 40-19.0 km.
 - We estimate the crust thinning occurs in 4 steps along the profile between the stations S003-S005, S007-S008 and S013-S014.
 - These 4 steps divided the area between the western plateau and the rift axis to four distinct regions of uniform crustal thickness.
 - A clear intra-crustal interface could be seen along the profile.

Primary conclusion:

- The crustal thinning occurs in discrete steps rather than gradual change especially along the southern profile.
- The crust thins from 38.0 km beneath the western plateau to 14 km (estimated from control source study) beneath the rift axis along the northern profile.
- The crust thins from 42.0 km beneath the western plateau to 19.8 km beneath the rift axis along the southern profile.
- The crustal thinning starts at the location of the high topographic escarpment along the two profiles (Fig. 8).
- The V_p/V_s ratio is evolving toward higher value for thinner crust and from north toward the south, indicating a change of crustal composition from felsic to mafic.
- Complex crustal structure with a clear anisotropy and probably dipping reflectors which involves more detailed study.
- Strong intra-crustal interfaces occurs beneath most of the stations and more clear along the southern profile (central Afar).
- We estimate a β of ~2.70 for the northern profile and β of 2.16 for the southern profile, indicating more evolved rifting in the North.

Acknowledgements

Data used in this study were collected by the AFAR17 project in Ethiopia. The instruments for the project were provided by the French National Research Infrastructure SISMOB-RESIF (http://www.resif.fr) and SES-UK. RESIF is supported by the Ministry of Higher Education and Research. The facilities of SES-UK are supported by the Natural Environment Research Council (NERC) under agreement R0110/64. Funding for fieldwork (deployments, data collection and maintenance) is from Sorbonne Université, ISTEP, Institut des Sciences de la Terre de Paris, Institut de Physique du Globe de Strasbourg (IPGS) and the PAUSE program. DK is supported by NERC grant NE/L013932/1, and MUR grant PRIN 201794972. We wish to thank the Addis Ababa University staff for help in customs clearance and for the technical facilities, the Ethiopian Regional authorities and local people for their kind cooperation and their help to make the fieldwork successful. We deeply thank, Alex Nercisson, CEE, Centre Français d'Etudes Ethiopiennes in Addis-Ababa for the help and support provided by the center during the experiment.

References

Buck W. R., Einarsson, P., & Brandsdóttir, R., 2006. J. Geophys. Res. 111:B12404, doi:10.1029/2005JB003879.
 Efron, B. and Tibshirani, R., 1986. The Bootstrap Method for standard errors, confidence intervals, and other measures of statistical accuracy. Stat. Sci., 1(1), 1-25.
 Grandin, R., Socquet, A., Doin, M. P., Jacques, E., de Chabaler, J. B. and King, G. C. P., 2010. Transient rift opening in response to multiple dike injections in the manda hararo rift (Afar, Ethiopia) imaged by time dependent elastic inversion of interferometric synthetic aperture radar data. J. Geophys. Res., 115, B09403, doi:10.1029/2009JB006883.
 Hammond, J. O. S., Kendall, J. M., Stuart, G., Keir, D., Ebinger, C., Ayale, A., and Belachew, M., 2011. The nature of the crust beneath the Afar triple junction: Evidence from receiver functions. Geochemistry, Geophysics, Geosystems, 12, Q12004. https://doi.org/10.1029/2011GC003738
 Makris, J. and Ginzburg, A., 1987. The Afar Depression: Transition between continental rifting and sea floor spreading. Tectonophysics, 141, 199-214.
 Stab, M., Belachew, M., P. R., Quiddeh, K., Ayalew, D. and Leroy, S., 2016. Modes of rifting in magma-rich settings: Tectono-magmatic evolution of Central Afar, Ethiopia. Tectonics, 35, 2-38. https://doi.org/10.1002/2015TC003893
 Wolfe, E., Ebinger, C., Yirgu, G., Renne, P. R. and Kelly, S. P., 2005. Evolution of a volcanic rifted margin: Southern Red Sea, Ethiopia. Geol. Soc. Am. Bull., 117, 846-864.
 Wright, T. J., Ebinger, C., Biggs, J., Ayale, A., Yirgu, G., Keir, D. and Stork, A., 2006. Magma-maintained rift segmentation at continental rupture in the 2005 Afar dyking episode. Nature, 442(7100), 291-294, doi:10.1038/nature04978.
 Zhu, L. and Kanamori, H., 2000. Moho depth variation in Southern California from teleseismic receiver function. J. geophys. Res., 105, 2969-2980.